Available online at www.sciencedirect.com
ScienceDirect
Polymer 48 (2007) 2087–2097
polymer
www.elsevier.com/locate/polymer

Analysis of crystal habits bounded by asymmetrically curved faces: Polyethylene oligomers and poly(vinylidene fluoride)☆

M.A. Shcherbina, G. Ungar*

Department of Engineering Materials, University of Sheffield, Mappin Street, Sheffield S1 3JD, UK

Received 10 August 2006; received in revised form 16 January 2007; accepted 7 February 2007
Available online 9 February 2007

Abstract

Curved lateral faces of lamellar polymer crystals have previously been described mathematically using a model of initiation and spreading of molecular steps on the growth surface. Previously it has been assumed that the steps spread with equal velocity v in both directions, and hence the model only applied to faces that have a two-fold axis or are bisected by a mirror plane normal to the lamella. Many lateral faces in polymer crystals do not have such symmetry. We recently solved the growth equation and reconstructed the growth profile for the case where the velocities in the left and right directions (v_l and v_r) are different, using a square lattice model. Here we adapt the model to oblique lattices suitable for {110} growth faces of polyethylene oligomers (ultralong alkanes) and PVDF. Very good fits are obtained with the observed unusual habits of crystals with curved {110} faces. It is shown that the shape of an asymmetric lateral crystal face is defined by two kinetic parameters, v_r/v_l and $il_0^2/(v_r+v_l)$, where i is the nucleation rate and l_0 the interchain distance in the growth plane. The value of v_r/v_l is found to be furthest from 1 at the smallest supercooling, which is consistent with the general principles of crystallization kinetics. The observed ten-fold difference between right- and left-moving steps on α-crystals of PVDF is attributed to the difference between edge-on and flat-on chain attachment at these steps, respectively. The high value of $il_0^2/(v_r+v_l)$, the cause of high curvature, gives a picture of a crystallization process that is only marginally nucleation controlled. Specific combinations of the above two parameters are predicted to produce exotic single crystals with re-entrant corners, so far unobserved.

Keywords: Crystal growth; Polymer crystallization; Morphology

1. Introduction

The observation of rounded single crystals [1,2] has played a major role in the understanding of the process of polymer crystallization. For example, Sadler's rough-surface theory of crystal growth was intended to describe crystallization at higher temperatures, where lateral crystal faces are above their roughening transition temperature T_R [3,4]. It was argued that the fact that the {100} faces in solution-grown polyethylene (PE) become curved at high temperatures indicates the presence of the roughening transition. In contrast, {110} faces with somewhat denser packing of surface chains and hence a higher interaction energy would have a higher T_R, hence the {110} faces remain faceted.

Nevertheless, subsequent detailed studies [5–7] have shown that the curvature of {100} faces in PE can be explained quantitatively by applying the Frank–Seto model of initiation and movement of steps [8,9]. Noticeable curvature occurs when the average step propagation distance is no more than two orders of magnitude larger than the stem width b.

However this approach cannot be applied to an ''asymmetric'' face, i.e. one that does not have a mirror plane bisecting the crystal normal to this face and to the lamellar plane, and also lacks a two-fold axis normal to the face. On the level of the unit cell, an asymmetric face must also lack the

☆ Part of this work has been published as communication in *Macromolecules* (Ref. [27]).

* Corresponding author. Tel.: +44 114 222 5457; fax: +44 114 222 5943.
E-mail address: g.ungar@shef.ac.uk (G. Ungar).

0032-3861/$ - see front matter © 2007 Elsevier Ltd. All rights reserved.
doi:10.1016/j.polymer.2007.02.009

associated glide plane and screw axis. Curved {110} faces of poly(vinylidene fluoride) (PVDF) and long alkane single crystals are examples of such asymmetric faces. Lozenge- and lens-shaped (lenticular) crystals of the orthorhombic α-form of PVDF have been observed which are bounded solely by curved {110} faces [10,11]. In PE, crystals bounded exclusively by {110} faces are confined to low crystallization temperatures T_c, where no curvature is observed. At higher T_c, where rounding occurs, {110} faces are truncated by curved {100} faces and they may disappear entirely [12]. We have recently carried out a systematic study of crystal habits of model long-chain monodisperse *n*-alkanes [13–15] and found that these compounds display most if not all the crystal habits encountered in PE. Moreover, unlike in PE, crystal lamellae bounded exclusively by {110} lateral faces were observed at high temperatures and low supercoolings in alkanes $C_{162}H_{326}$ and $C_{198}H_{398}$ [16–18]. While faceted {110}-bounded lozenges grow from octacosane, similarly nontruncated crystals are formed from 1-phenyldecane and methylanthracene, but with characteristically asymmetrically curved {110} faces; these faces are almost straight near the acute corners of the lozenge and substantially curved near the obtuse corners.

The above observations motivated us to propose a modification of Frank–Seto equations by assuming that the rates of propagation of left and right steps on the growth surface are different [16]. In the preceding paper [19] we solved the appropriate differential equation of the secondary nucleation model with moving face boundaries, using a simple square lattice model. In the present publication we adapt the model to a general oblique 2D lattice suitable in principle for the description of all asymmetric growth faces. Specifically we then adopt the geometrical parameters appropriate specifically to the calculation of {110} faces of orthorhombic crystals of PE, *n*-alkanes and PVDF. We then compare the derived profiles with those observed experimentally. This makes it possible to determine hitherto unavailable kinetic parameters, i.e. the individual propagation velocities of right and left steps, and the initiation (secondary nucleation) rate on asymmetric crystal face.

2. Theoretical construction of lateral habit of a single crystal

2.1. Growth front profile on a simple square lattice

The Frank–Seto treatment [8,9] starts from a surface nucleation event creating a pair of steps. The nucleation rate is i nuclei per unit edge length per unit time, and the steps travel to the left and right at an equal average net rate v (in units of length per time). The advance of patches of stems on the substrate is arrested either by the collision between left-moving and right-moving steps, or by the patches reaching the end of the crystal face. If $l(x, t)$ and $r(x, t)$ are the densities of left and right steps, respectively, in the vicinity of position x along the substrate of length L, two flux equations must be satisfied:

$$\frac{\partial r}{\partial t} = -v\frac{\partial r}{\partial x} + i - 2v\,lr$$
$$\frac{\partial l}{\partial t} = +v\frac{\partial l}{\partial x} + i - 2v\,lr \tag{1}$$

These equations describe the local variation in concentration as a result of drift, creation and annihilation processes, expressed by the first, second and third terms on the right, respectively.

Assuming that no step enters from outside, and that the substrate length increases simultaneously with the advance of the growth front, with the substrate ends moving outward at a net rate h, boundary conditions for the Eqs. (1) are:

$$r(-ht, t) = 0$$
$$l(ht, t) = 0 \tag{2}$$

In the case of {100} growth in PE for example, h is determined by the growth rate of adjacent {110} faces. Mansfield [6] first obtained solutions of the above equations, deriving the growth face profile $y(x, t)$. Such $y(x, t)$ describes adequately the observed [5,12] and simulated [20] shapes of {100} faces of single crystals of polyethylene and, as found recently [13–15], long alkanes. $y(x)$ defines an ellipse if a square lattice is used [6], even though this is not strictly true for very small crystals [7,19]. The ellipse becomes leaf-shaped when transposed onto a polyethylene-like centred rectangular lattice [21]. The {100} face is defined as part of this ellipse when the substrate edge moves at a rate $h < v$, i.e. in the case of a truncated lozenge crystal. On the other hand, if $h > v$, the outer parts of the {100} face are described by straight non-crystallographic faces tangent on the central elliptical section [5,7].

An alternative derivation of the growth profile of lamellar polymer crystals, also based on Eqs. (1), has been proposed by Point and Villers [7]. According to these authors, their equations are equally applicable to the secondary nucleation and the rough-surface growth mechanism. In actual fact, the curved growth face shape obtained by Point and Villers is very close to that obtained by Mansfield. Only for very small crystals, typically below 0.1 μm, a correction is significant [19].

More recently the growth habit of PE crystals has been treated using a nonlinear reaction diffusion equation where the crystal–melt interface was diffuse rather than sharp (zero thickness) [22]. The equation is solved numerically and, among other things, this avoids the problem of moving boundaries. It may be mentioned in passing that the solution of the reaction diffusion equation in the form of a solitary wave has been applied to long alkanes to describe the propagation of the ''dilution wave'' through the crystallizing solution [23].

Returning to the Frank–Seto model, for asymmetric faces Mansfield's treatment must be modified taking into account the different rates of stem attachment to the right and left ends of the growing patch of stems (Fig. 1). In the case of {110} face of PE, there would be no difference between the steps and between their propagation rates if the lattice had

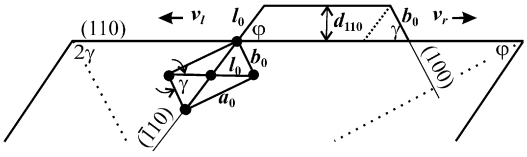

Fig. 1. View along the chain axis of a new molecular layer deposited on a {110} growth face of polyethylene showing the asymmetry of steps. A unit cell is shown for reference.

hexagonal symmetry, i.e. if the ratio of lattice parameters $a_0/b_0 = \sqrt{3}$; in that case the right and left steps would be equivalent, both having an angle of 120°. However, in the orthorhombic lattice of PE the two step angles γ and φ differ by 11°, while for PVDF (α-form) they differ by 8° − see Table 1. Similarly, in PE, the distance between adjacent chains in the {100} plane (length of the right-hand edge, equal to b_0) is shorter than the distance in the {110} plane l_0 (length of the left-hand edge). The reverse is true for the α-form of PVDF. These differences would be expected to produce some difference in either the molecular attachment or detachment rates, or both. With reference to Fig. 1, Eqs. (1) become

$$\frac{\partial r}{\partial t} = -v_r\frac{\partial r}{\partial x} + i - (v_r + v_l)\, lr$$
$$\frac{\partial l}{\partial t} = +v_l\frac{\partial l}{\partial x} + i - (v_r + v_l)\, lr \tag{3}$$

Assuming that the spreading rates of substrate edges h_r and h_l can differ, we have solved [19] the system of differential Eqs. (3) with the following boundary conditions:

$$r(-h_l t, t) = 0$$
$$l(h_r t, t) = 0 \tag{4}$$

The resulting functions $r(x, t)$ and $l(x, t)$ were used in the reconstruction of the shape of the growth face on the simple square lattice by integration of the mean slope of a growing face given by the equation:

$$\frac{\partial y}{\partial x} = b(l - r) \tag{5}$$

where b is the width of a single chain (side of the unit square). This gives for the profile of the growth front:

$$y = 2bt\sqrt{\frac{i}{v_r + v_l}}\sqrt{(v_r - x/t)(v_l + x/t)} \tag{6}$$

We can rewrite the above equation in standard quadratic form for time-independent coordinates $X_s = x/t$ and $Y_s = y/t$:

Table 1
Crystal lattice parameters, interchain distances and angles for orthorhombic PE and PVDF (α-form) (cf. Fig. 1)

	PE, long alkanes	PVDF
a_0	7.40 Å	9.64 Å
b_0	4.93 Å	4.96 Å
$l_0 = 1/2(a_0^2 + b_0^2)^{1/2}$	4.45 Å	5.42 Å
γ	56.3°	62.8°
φ	67.2°	54.5°

$$\left[\frac{X_s - \frac{v_r - v_l}{2}}{\frac{v_r + v_l}{2}}\right]^2 + \left[\frac{Y_s}{b\sqrt{i(v_r + v_l)}}\right]^2 = 1 \tag{7}$$

Eq. (7) is the equation of an ellipse with the centre shifted by $(v_r - v_l)/2$ along the x-axis. In the present paper we adapt this solution to oblique 2D lattices suitable for describing asymmetrically curved {110} faces of orthorhombic crystals such as those of PE and PVDF, and compare the calculated crystal habits with those observed experimentally.

It should be emphasised that, as shown before [19], the proposed approach is valid for crystals larger than ca. 0.1 μm, which includes the vast majority of polymer single crystals observed by the usual microscopic techniques. For smaller crystals the validity of the entire approach becomes questionable, due to the small number of sites involved. It should be noted further that the approximations used in the Frank–Seto model (e.g. neglect of multiple-height steps and of step bunching) make the treatment less quantitatively accurate for faces of higher curvature.

2.2. Transposing the solution to an oblique lattice

Solutions based on a simple square lattice could be directly applied only to tetragonal crystals. In order to apply Mansfield's solution [6] to the growth of the symmetric {100} face of polyethylene [21] and long n-alkanes [14,15], it had to be transposed onto a centred rectangular lattice, where the x-axis is parallel to the {100} plane, i.e. to the crystallographic b-axis. For this case one could consider the sides of the kinks to be tilted at an angle γ to the facet plane. The kink sides are densely packed planes, in this case the {110}. Thus for the {100} growth plane, as an example of a symmetrical growth face, the following are the relationships between the reduced coordinates of the simple square (X_s, Y_s) and the centred rectangular lattice (X_c, Y_c) (cf. Ref. [21]):

$$Y_c = \frac{a_0}{2b_0} Y_s$$
$$X_c = X_s + \left[\frac{a_0}{2}\sqrt{2i\nu} - Y_c\right]\cot\gamma \tag{8}$$

For an asymmetric face these relationships must be modified by taking into account the difference between the tilt angles of right and left kinks, and between the propagation velocities in the two directions. Angles γ and φ can be derived from the known unit cell parameters for PE [24] and PVDF [25,26] (Table 1). We have to consider the two branches of the growth front separately, either side of the maximum point at $X = (v_r - v_l)/2$. The two branches must meet at that point for the sake of smoothness of the growing face. Hence (cf. Fig. 1b in Ref. [27]):

$$Y_{ob} = \frac{d_{110}}{l_0} Y_s;$$
$$X_{ob} = X_s - \left[d_{110}\sqrt{i(v_r + v_l)} - Y_{ob}\right]\cot\varphi \quad \text{if } X < \frac{v_r - v_l}{2};$$
$$X_{ob} = X_s + \left[d_{110}\sqrt{i(v_r + v_l)} - Y_{ob}\right]\cot\gamma \quad \text{if } X \geq \frac{v_r - v_l}{2}; \tag{9}$$

here d_{110} is the {110} interplanar spacing.

2.3. Construction of lozenge-type crystal shapes with asymmetrically curved faces

Single crystals of PE bounded exclusively by straight {110} faces (“lozenges”) grow only from solutions at relatively *low* crystallization temperatures T_c (e.g. 70 °C) [12,28]. As T_c is raised, {110} faces become truncated by intervening {100} faces, which become curved as T_c is increased further. The exact curvature of {110} faces cannot be studied as these faces diminish and disappear at the highest T_c. However, in very long alkanes, using solvents like *n*-octacosane, nontruncated {110} lozenges can also be obtained from solutions at the *highest* T_c, i.e. at the lowest supercoolings − e.g. $C_{198}H_{398}$ at 108 °C or $C_{162}H_{326}$ at 105 °C [16]. As discussed in Ref. [15], these are the conditions where growth is least affected by self-poisoning. Furthermore, by changing the solvent to 1-phenyldecane or methylanthracene, for the first time nontruncated {110}-bounded crystals with *curved* {110} faces were observed [16,18]. As mentioned in Section 1, similar crystals appear also in PVDF [10,11]. The unusual asymmetric curvature of {110} faces has led us to propose that the rates of right- and left-moving steps (kinks and antikinks) are different [16,19]. In this section we build the whole shape of a PE/alkane single crystal with nontruncated curved {110} faces.

Let us consider the formation of a lozenge crystal of PE. Four {110} faces grow from a common centre. If the ratio between step initiation and propagation rate is low, the faces are flat (Fig. 2a). The two crossed dotted lines in Fig. 2a and b define the baselines ($t = 0$), or x-axes, used in the description of growth of the four {110} faces. For a low initiation-to-propagation ratio, the growth faces are not only straight, but also parallel to their baseline (Fig. 2a). Thus such facets maintain crystallographic angles at the apices.

As the ratio of step initiation and propagation rates increases, the faces become curved, cease to be parallel to the baseline and the apex angles change as they are defined by the intersection of adjacent growth faces − see Fig. 2b. Since the growth of each individual {110} plane is affine [19], the crystal growth is also affine under the conditions of constant temperature and solution concentration. The initiation and propagation rate ratio is defined here as the dimensionless ratio $il_0^2/(v_r + v_l)$, where l_0 is the spacing between chains in the growth {110} plane. This important dimensionless parameter gives the ratio of probabilities of deposition of a stem as a secondary nucleus against the probability of its attachment to a niche on either side of a spreading layer.

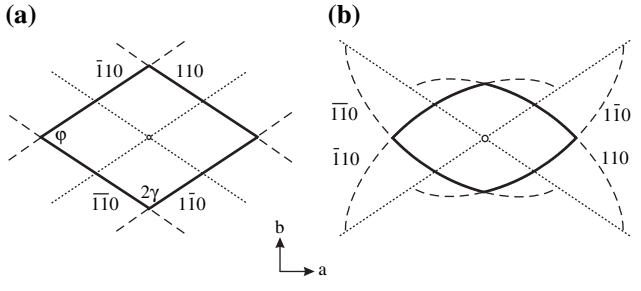

Fig. 2. Construction of the crystal shape bounded by four (a) straight and (b) curved {110} crystal growth faces (alkane/PE lattice parameters are used). Bold lines are growth fronts intersecting at the corners of the crystal. The boundaries of the faceted lozenge crystal in (a) are parallel to the baseline reference $t = 0$ planes (dotted lines). The curved growth profile in (b) was calculated using Eqs. (7) and (9) with parameters $il_0^2/(v_r + v_l) = 0.1$ and $v_r/v_l = 2$.

To avoid confusion regarding the meaning of “right” and “left”, we adopt the convention that, viewing the crystal flat-on and with the relevant $hk0$ growth face on top, “right” is the right direction along that face if h and k are both positive or both negative. With the crystal *oriented as in Fig. 2*, v_r thus refers to the spreading rate to the right for (110) and $(1\bar{1}0)$ faces, and to the left for $(\bar{1}10)$ and $(\bar{1}\bar{1}0)$ faces.

Part of the library of crystal shapes, constructed in the way described in Fig. 2b, is shown in Fig. 3. Note that the crystals in Fig. 3 are rotated by 90° relative to those in Fig. 2. As expected, the curvature of the growth faces is higher, the higher the initiation/propagation rate ratio $il_0^2/(v_r + v_l)$ (cf. Fig. 3 first and fourth rows). On the other hand, increasing the asymmetry of growth has the effect of extending the crystal along one of the lozenge diagonals; i.e. for $v_r < v_l$ the crystal extends along the b-axis (left-hand columns in Fig. 3), while for $(v_r > v_l)$ the crystal extends along the a-axis (right-hand columns). For moderately low initiation/propagation ratios the curvature may not be noticeable, yet an apparently faceted growth face could be tilted relative to its crystallographic baseline, particularly if the difference between v_l and v_r is large (e.g. crystals at the bottom left and bottom right corners of Fig. 3). The latter effect may result in “non-crystallographic facets” or even in misleading indexing of crystal faces. In a separate publication we deal with such an example in the case of poly(ethylene oxide) [29].

The “curvature” of the growth face, defined here as the length ratio of the short (L_y) and long (L_x) axes of the ellipse, can be expressed in terms of the propagation-to-initiation ratio as follows. For the simple square lattice of unit cell parameter b:

$$\frac{L_y}{L_x} = b\sqrt{\frac{2i}{v}} \tag{10a}$$

For the centred rectangular lattice (symmetric growth), specifically {100} face of PE or PVDF:

$$\frac{L_y}{L_x} = \frac{a_0^2}{2b_0}\sqrt{\frac{i}{2v}} \tag{10b}$$

For an oblique lattice (asymmetric growth), specifically {110} face of PE or PVDF:

$$\frac{L_y}{L_x} = \frac{2d_{110}^2}{l_0}\sqrt{\frac{i}{v_r + v_l}} \tag{10c}$$

These expressions give the link between the dimensionless initiation/propagation rate parameter such as $il_0^2/(v_r + v_l)$ and the shape of the growth front. At the same time, the effect of growth asymmetry, i.e. of $v_r \neq v_l$, is to shift the ellipse

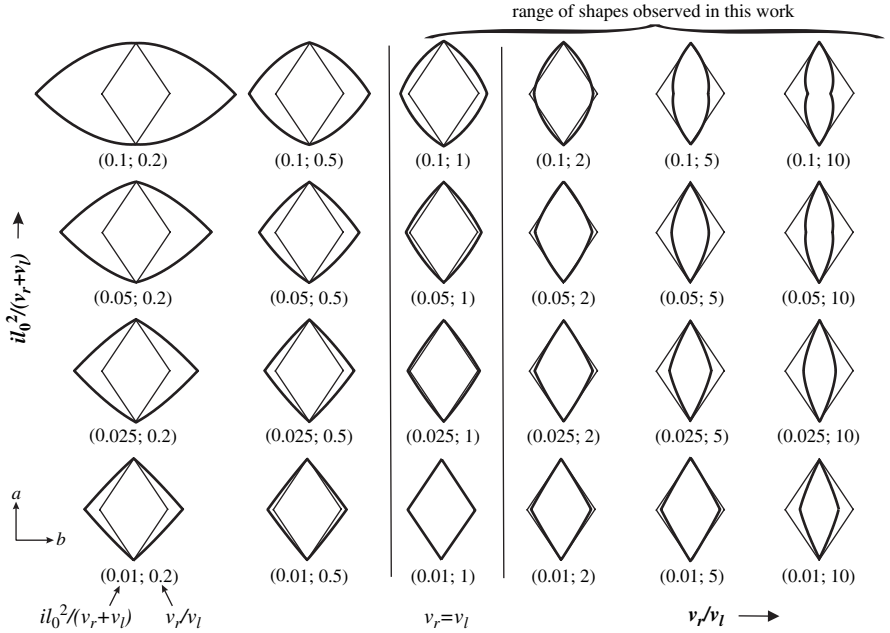

Fig. 3. Constructed shapes of PE crystals bounded by {110} faces. Rows: shapes with the same initiation/propagation rate ratio $il_0^2/(v_r + v_l)$; columns: shapes with the same right/left propagation rate ratio v_r/v_l. For comparison, crystallographic lozenges with the same size in the *a* direction are superimposed (thin lines). *a*-Axis is vertical and *b*-axis horizontal. The corresponding kinetic parameters are shown beneath each simulated crystal in the form $(il_0^2/(v_r + v_l); v_r/v_l)$. The shapes in the 3rd column are for symmetric growth ($v_r = v_l$).

along the crystallographic growth plane, i.e. along the *x*-axis, by $(v_r - v_l)/2$.

The peculiar case of crystals with re-entrant (concave) corners ($2\gamma > 180^\circ$ − see top right in Fig. 3) will be discussed briefly further below.

3. Comparison of experimental and theoretical crystal habits

3.1. Long alkanes

As mentioned in Section 1, nontruncated lozenge shape with more or less curved {110} edges and with apex angles different from those crystallographically predicted have been observed experimentally in extended-chain crystals of long alkanes $C_{198}H_{398}$ and $C_{162}H_{326}$ when grown from solution in 1-phenyldecane [16]. The value of the acute angle φ was found to increase above the crystallographic value of 67° with decreasing crystallization temperature, reaching 84° at 92.4 °C, i.e. at 9.7 °C supercooling. This trend was accompanied by a deviation of the width-to-length ratio l_b/l_a from the ideal value of $0.662 = \tan(\varphi/2)$. Fits of theoretical shapes to the observed $C_{162}H_{326}$ single crystals in Ref. [16] are shown in Fig. 4.

Recent investigations have shown that lozenges with asymmetrically curved {110} faces are a widespread occurrence in

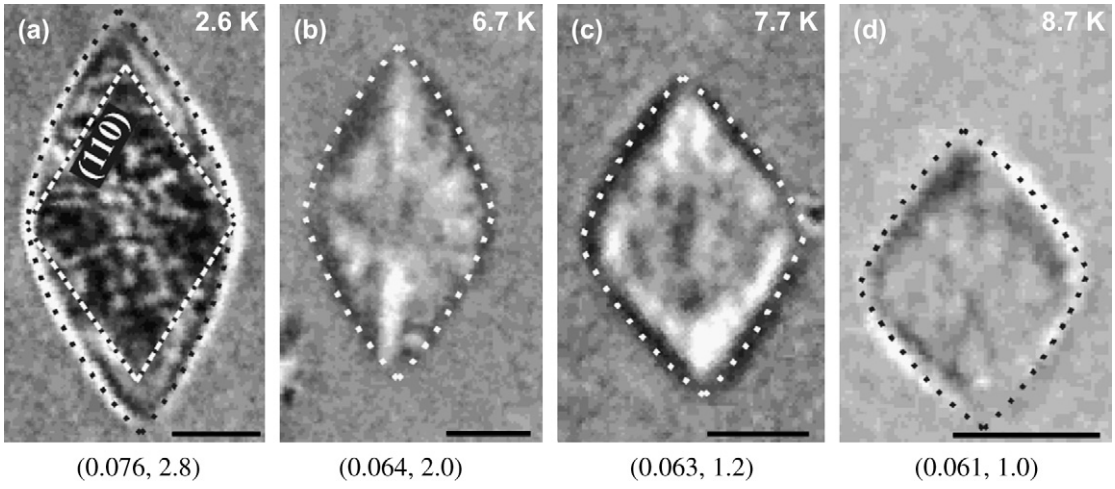

Fig. 4. Interference optical micrographs of single crystals of extended-chain long alkane $C_{162}H_{326}$ grown from 1% (wt) solution in 1-phenyldecane at the supercoolings (ΔT) indicated. In all cases the crystallographic *a*-axis is vertical and *b*-axis horizontal. Fitted shapes are overlaid (dotted lines). Fitting parameters beneath each micrograph are shown in the format: $(il_0^2/(v_r + v_l); v_r/v_l)$. Scale bar is 10 μm. A faceted {110}-bound lozenge is inscribed in the crystal in (a).

long alkane single crystals grown from solutions in aromatic solvents at low supercoolings. Fig. 5 shows a series of crystals of $C_{198}H_{398}$ from methylanthracene solution grown and observed at a range of temperatures. 2-Methylanthracene was purchased from Sigma–Aldrich. To grow the crystals, the low vapour pressure solution, sandwiched between glass coverslips, was transferred rapidly from the T_1 to the T_c hot stage of a custom-designed Linkam T-jump microscope stage, T_1 being above the extended-chain dissolution temperature and T_c being the selected crystallization temperature. The growing crystals were digitally recorded using an interference contrast Olympus BX50 microscope. For more experimental details see Ref. [15].

As seen in Fig. 5, for supercoolings less than 5 °C the crystals are bounded exclusively by {110} faces. The acute angle of the {110} lozenge clearly increases with supercooling, as shown in Fig. 6. A similar trend of increasing angle, with crystals approaching a square shape, was observed previously for $C_{162}H_{326}$ in 1-phenyldecane [16]. The fact that the crystals at $\Delta T = 3$ °C have their φ angle equal to the crystallographic value is purely coincidental, and is the result of cancellation of the effects of step rate asymmetry and face curvature. In all cases the {110} faces could be fitted well with growth profiles calculated on the basis of asymmetric step propagation.

At supercoolings higher than 5 °C the acute angle of the crystal disappears as the lozenge gets truncated by {100} faces. With ΔT increasing further, {100} faces become more pronounced at the expense of {110}. The shapes of the predominantly {100}-bounded crystals grown from octacosane solutions of a wide range of long alkanes have been studied in considerable detail [13–15] and kinetic parameters such as step nucleation and propagation rates, i and v, were found to vary remarkably with small changes in temperature. This temperature sensitivity was interpreted in terms of the self-poisoning effect close to growth transitions such as extended- to folded-chain, once- to twice-folded chain etc.

3.2. Poly(vinylidene fluoride)

As mentioned in Section 1, lenticular (lens-shaped) crystals bounded solely by curved {110} faces are also observed in poly(vinylidene fluoride). These crystals display a range of habits, from lozenge with perfect crystallographic facets to lens-shape with the acute angle completely rounded out. Fig. 7 presents electron micrographs [11] of selected PVDF crystals grown from melt and from blends with poly(ethyl acrylate). Calculated growth profiles are fitted, using the fitting parameters indicated.

The PVDF crystals are orthorhombic (α-form), with the lattice parameters given in Table 1. Note that, while the a_0/b_0 ratio in polyethylene is 1.50, i.e. less than the hexagonal lattice value of $\sqrt{3}$, in PVDF the a_0/b_0 ratio is 1.94, i.e. larger than the hexagonal value. Thus the asymmetry of {110} faces can be said to be reversed. For example, while in PE the interchain distance in the {110} plane, l_0, is shorter than the distance b_0 in the {100} plane, the opposite is true in PVDF. The values of angles γ and φ between crystallographic {110} facets in PVDF are also given in Table 1.

The observed variety of lateral crystal habits of PVDF can be well accounted for by the crystal shapes constructed according to the present theory. In spite of the "reversed" distortion of the hexagonal unit cell in PVDF, both in alkanes and in PVDF the v_r/v_l ratio of step velocities is greater than 1, i.e. steps move faster toward the acute angle of the lozenge than away from it – see below.

3.3. Experimental determination of step initiation and propagation rates

As is shown above by a number of examples, the proposed theory of asymmetric spreading of molecular layers on {110} growth faces describes well the shape of different orthorhombic polymer single crystals, grown from either solution or melt. Libraries of simulated crystal shapes, such as that in Fig. 3, can be easily produced for any polymer with a known unit cell, single crystals of which are bounded by asymmetric growth faces belonging to the same class. Thus, by finding the simulated crystal shape that matches the shape of a real crystal, we obtain the values of $il_0^2/(v_r + v_l)$ (dimensionless ratio of step initiation rate to the average step propagation velocity) and v_r/v_l (the ratio of velocities of right- and left-moving steps). Further, by measuring the macroscopic growth rates perpendicular to the growth faces, one can obtain the absolute values of i, v_r and v_l.

In cases where more than one class of planes define the lateral crystal habit (e.g. {110} and {100} in PE under appropriate conditions, {120} and {100} in PEO [30]), only the relevant part of the crystal should be fitted by the present method. To obtain the initiation/propagation ratio for symmetric faces, such as {100} in PE or PEO, the methods of Mansfield [6] or Point–Villers [7] should be used corrected for the appropriate lattice type [21]. Both the {110} and {100} faces were fitted to the sequence of alkane crystals in Fig. 5. Because of the relatively low spatial resolution of the optical micrographs in question, both sets of faces could not be analysed reliably on the same crystal, since only a relatively short portion of each face is visible. However, in micrographs of higher resolution (TEM, AFM), the better definition of the shape should allow fitting of shorter sections of each face and allow the determination of step initiation and propagation rates in a wider temperature range. Similarly, melt crystallization, which often produces larger single crystals [31], is amenable to extensive studies of habits by optical microscopy.

It should be noted that two dimensionless parameters are needed to define completely the lateral shape of a single crystal bounded by one class of asymmetric planes. In contrast, only one parameter is sufficient for crystals delineated by *symmetric* planes of a single class. If two different classes of planes define the crystal, additionally the ratio of growth rates of the two classes of planes must be defined in order to describe the lateral habit completely. Thus, e.g., the complete shape of a truncated lozenge of PE is defined by four parameters, the fourth being the ratio of growth rates of the two face

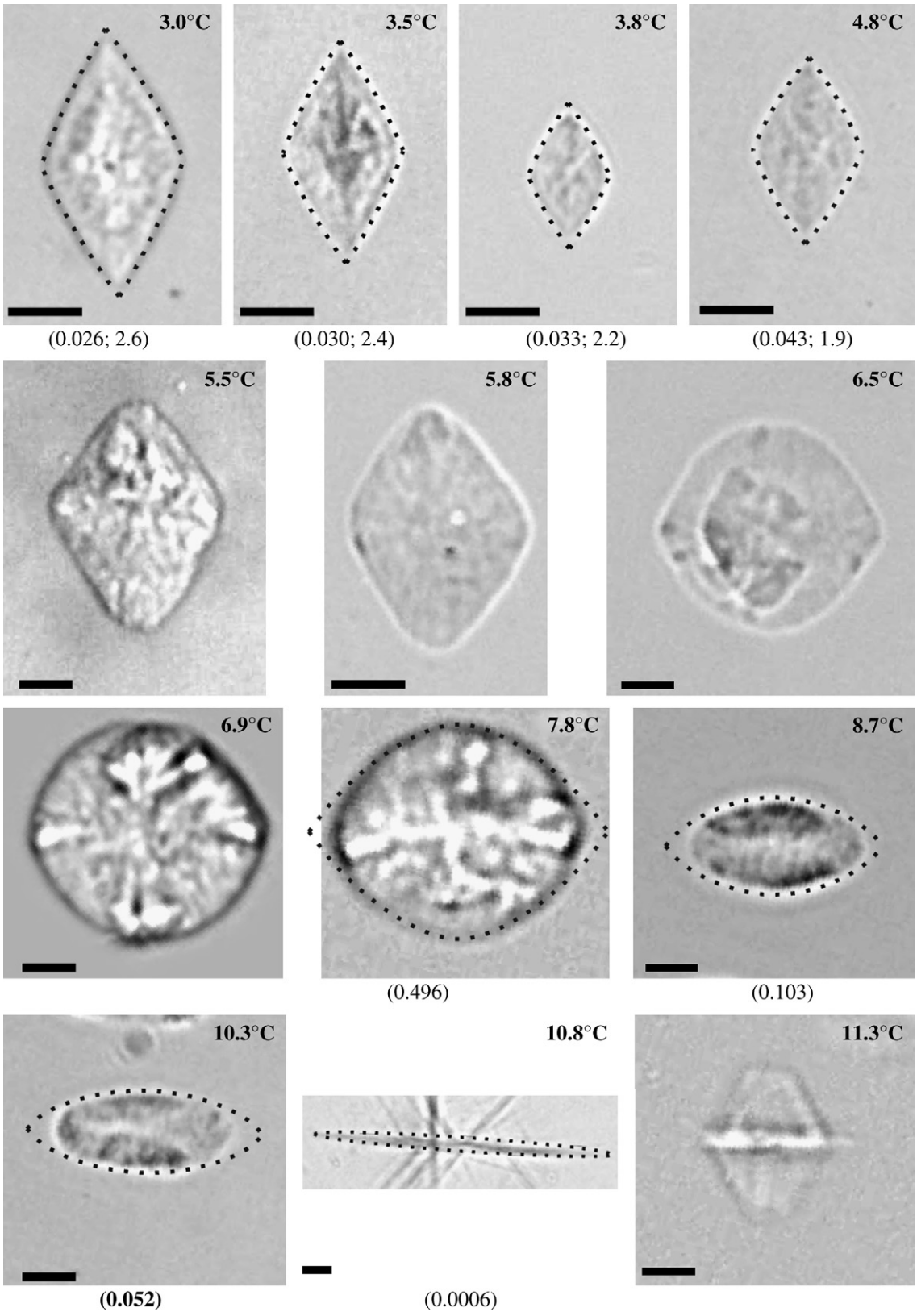

Fig. 5. Interference contrast micrographs of single crystals of long alkane $C_{198}H_{398}$ grown from 2% (wt) solution in methylanthracene at different supercoolings indicated. For reference, the dissolution temperature of extended-chain crystals is 111.7 °C. In all cases the crystallographic *a*-axis is vertical and *b*-axis is horizontal. Fits to theoretical {110} lozenges (top row) and {100} Mansfield ellipses (two bottom rows) are shown by black dotted lines where such fits are meaningful. The parameters used are shown beneath each micrograph in the format $(il_0^2/(v_r + v_l);\ v_r/v_l)$ for {110} faces, and $(ib_0^2/2v)$ for {100} faces. The crystal at $\Delta T = 11.3$ °C is once-folded chain, all others are extended-chains. *a*-axis vertical. Bar = 10 μm.

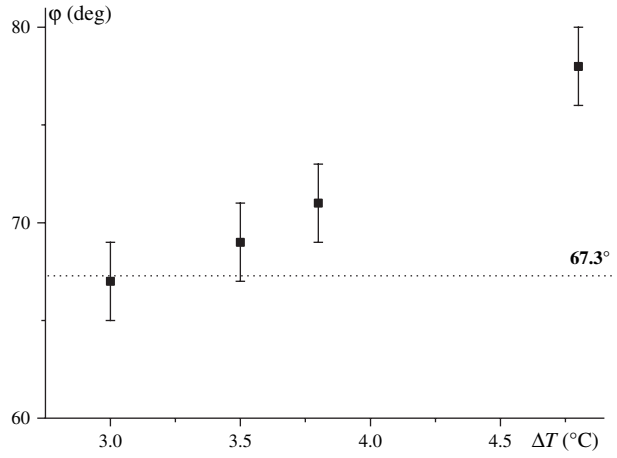

Fig. 6. Supercooling dependence of the acute angle φ for extended-chain non-truncated lozenge crystals of alkane $C_{198}H_{398}$ grown from 2% (wt) solution in methylanthracene. The dotted line indicates the crystallographic value of φ.

types G_{110}/G_{100}. Here $G_{110} = d_{110}\sqrt{i(v_r + v_l)}$ and $G_{100} = (a_0/2)\sqrt{2iv}$.

It should be noted that the determination of the two dimensionless parameters, $il_0^2/(v_r + v_l)$ and v_r/v_l, can involve a degree of ambiguity. As seen in Fig. 3, there exist some pairs of parameters which give very similar crystal shapes (see, e.g. crystals (0.01; 0.2) and (0.025; 0.5)). However, examining extended temperature or concentration dependencies of crystal shapes can reduce the ambiguity considerably (Section 3.5).

3.4. Asymmetry of patch spreading as a function of supercooling

Fig. 8 shows the dependencies on supercooling of the two kinetic parameters, v_r/v_l and $il_0^2/(v_r + v_l)$, for {110} faces for single crystals of alkanes $C_{162}H_{326}$ and $C_{198}H_{398}$. Crystals presented, respectively, in Fig. 4 and Fig. 5 (top row) were used in the fitting.

The results obtained are consistent with physical principles of crystal growth. The difference between the propagation rates of right- and left-moving steps is the greatest near the dissolution temperature T_d, and decreases with increasing supercooling. This is understandable: at T_d (or at melting temperature T_m) molecular attachment and detachment rates are balanced and any small difference in kinetic conditions between the right and the left steps would have the greatest impact near T_d (T_m). The question then arises whether it is the attachment or detachment rate that differs. Detachment rate is determined primarily by the binding energy of the affected stem. It can be shown that, due to glide plane symmetry, the binding energies of chains attached at the right and left steps on a {110} face in e.g. PE are equal – see Fig. 9. Hence the average detachment rates of chains at the two ends of a surface patch are equal. It therefore follows that the difference between v_l and v_r arises from the difference in *attachment* rates. This, one would assume, is related to the steric conditions of chain attachment into the two non-equivalent niches. The two adjacent chains on the side of the left step, separated

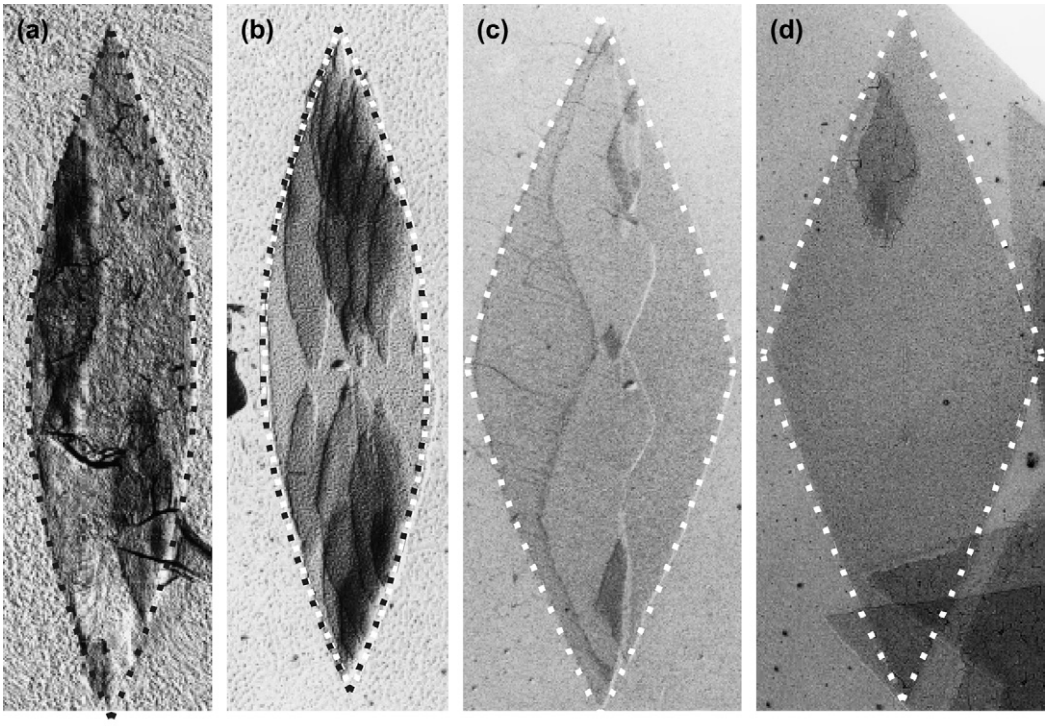

Fig. 7. Electron micrographs of poly(vinylidene fluoride) crystals (α-form), reproduced from Ref. [11]. (a) Crystallized from melt at 172 °C, (b–d) crystallized from blends with poly(ethyl acrylate): (b) at 172 °C, 30% PVDF, (c,d) −150 °C, 0.5% PVDF. Fits of {110} faces using simulated crystal shapes are shown with dotted lines. Below each micrograph fitting parameters are given in the form ($il_0^2/(v_r + v_l)$; v_r/v_l).

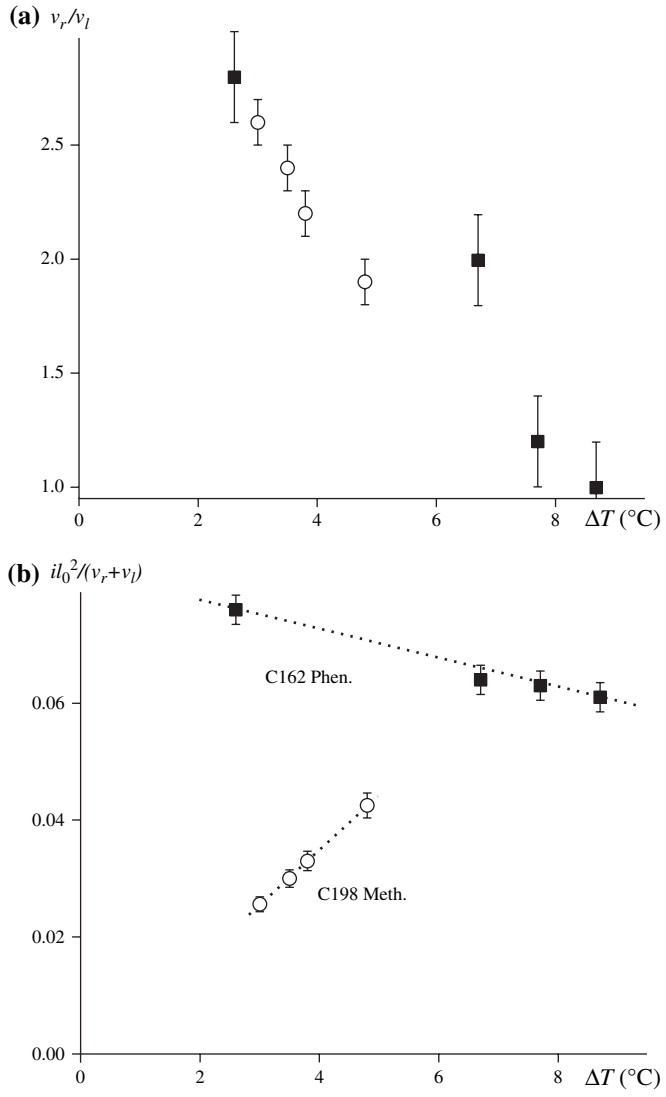

Fig. 8. Supercooling dependencies (a) of the ratio of right to left step propagation velocities v_r/v_l and (b) of the dimensionless ratio of initiation rate to the combined step propagation rate $il_0^2/(v_r+v_l)$ for two long alkanes: $C_{198}H_{398}$ grown from 2% (wt) solution in methylanthracene (hollow circles) and $C_{162}H_{326}$ grown from 1% (wt) solution in 1-phenyldecane (solid squares).

by l_0, always have different setting angles, while those on the side of the right-hand step, separated by b_0, have the same setting angle. Incidentally, because of the alternating setting angles of chains along the {110} face, the *average* attachment rate of two end chains must be considered at each end.

Compared to that in alkanes, the asymmetry of step propagation is even larger on {110} faces of PVDF. The crystals in Fig. 7a and b have a v_r/v_l ratio of 10 and 9.5, respectively. A schematic representation of the structure at the {110} face of a PVDF crystal, with a three-stem-wide layer attached, is shown in Fig. 10. Although the *Pc2m* space group, associated with this structure [26], does not have a glide or screw along either *a* or *b*, averaging the two alternating chains (actually four, if up–down disorder is considered) at the right or the left step, makes their binding energies equal, as in the case of PE. Thus, again we have to attribute the difference between

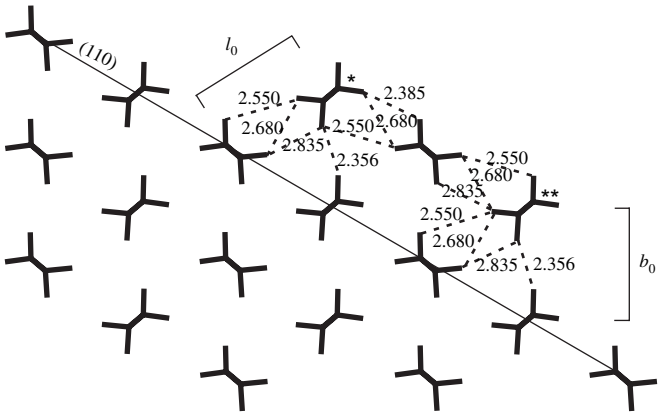

Fig. 9. {110} Edge of an orthorhombic PE/alkane crystal with a surface patch of three chains, viewed along the chain axis. The energy of the molecular cluster was minimised using Cerius-2 (Open Force Field). Interatomic distances between closest hydrogens on nearest neighbour chains are indicated in Angstroms for the chains at the left (*) and right (**) ends of the patch. As the distances for the two chains are identical, their van der Waals binding energies are also equal.

v_r and v_l to the difference in attachment rates. The fact that v_r is up to 10 times faster than v_l must be associated with the considerable difference in the way attaching chains slot into the two non-equivalent niches. Approximating the *tgtg′* carbon backbone of an incoming chain as a ribbon, a chain approaches the right-hand niche edge-on, while it approaches the left-hand niche flat-on. Even a qualitative consideration would thus suggest a larger asymmetry of spreading rates in PVDF, compared to that in PE and the alkanes. Finding the reason that edge-on attachment is faster than flat-on one could be the subject of a molecular simulation study.

3.5. Temperature dependence of the initiation/propagation ratio

Fig. 8b shows the experimental dependence of the dimensionless ratio of initiation and propagation rates $il_0^2/(v_r+v_l)$ on supercooling. While for $C_{198}H_{398}$ grown from methylanthracene solution the ratio increases with ΔT, for $C_{162}H_{326}$

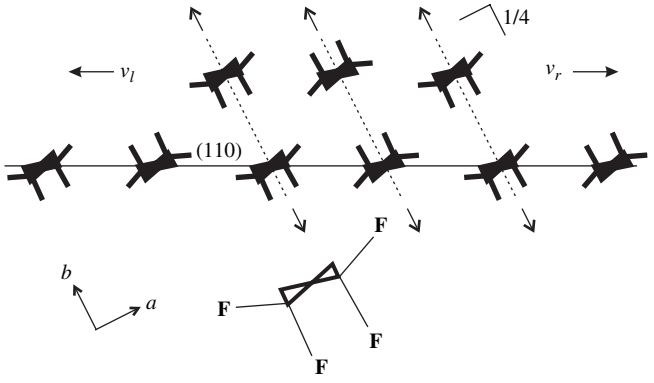

Fig. 10. {110} Surface of the orthorhombic α-form of PVDF [26], viewed along *c*-axis, including a deposited three-chain patch. Polymer chains in their *tgtg′* conformation are represented by symbols, one of which is expanded at the bottom, showing C–C (thick) and C–F (thin) bonds, with C–H bonds omitted. The symmetry elements of the *Pc2m* space group are also shown.

from 1-phenyldecane the ratio appears to decrease. In fact, by nature $il_0^2/(v_r + v_l)$ is bound to increase in all cases at very small undercoolings, so long as crystallization is even mildly nucleation controlled. Since in that case the barrier for deposition of the first stem is higher than the barrier for subsequent stems, a small ΔT may be sufficient to allow propagation but not nucleation, making $il_0^2/(v_r + v_l) \to 0$ as $\Delta T \to 0$.

The question is then why the nucleation/propagation ratio for $C_{162}H_{326}$ apparently decreases with increasing ΔT. To answer this we recall the temperature dependence of the equivalent ratio $ib_0^2/2v$ for the growth of {100} faces, which in all long alkanes studied passes through a maximum between the dissolution temperatures of extended and once-folded chains (see Ref. [15] and Fig. 25 in Ref. [17]). There is a similar maximum between T_d's of once- and twice-folded chains [15]. The position of the maximum within the interval varies. The fact that for {100} faces $ib_0^2/2v \to 0$ as T_d of folded chains is approached from above indicates that, for {100} growth, nucleation is far more inhibited by self-poisoning than propagation. Since we cannot follow the behaviour on {110} faces all the way down to T_d of folded chains due to crystal truncation, we cannot say whether $il_0^2/(v_r + v_l) \to 0$ as T_d of folded chains is approached. However there clearly is the observed decrease in $il_0^2/(v_r + v_l)$ with increasing ΔT for {110} growth of $C_{162}H_{326}$ crystals (Fig. 8b). We believe that the maximum is either below $\Delta T = 2.5\ ^\circ C$ or somewhat above that value. In contrast, for $C_{198}H_{398}$ crystals from methylanthracene, the maximum, if there is one, must be beyond $\Delta T = 5\ ^\circ C$.

3.6. Possibility of re-entrant corners

The predicted crystal shape at the top right of Fig. 3 shows re-entrant (concave) corners in the place of the obtuse corners of the lozenge. This unusual morphology is predicted to occur under rather exotic conditions of high asymmetry of patch spreading (v_r/v_l far from 1) and, at the same time, high initiation-to-propagation ratio $il_0^2/(v_r + v_l)$. As discussed above, the two conditions are to some extent mutually exclusive. It is at the smallest supercooling that we expect the largest deviation from $v_r/v_l = 1$, but it is also as $\Delta T \to 0$ that $il_0^2/(v_r + v_l) \to 0$. However, as seen in Fig. 8b for $C_{162}H_{326}$, $il_0^2/(v_r + v_l)$ can reach quite a high value at low ΔT. PVDF is in fact a good candidate to look for the habit with re-entrant corners, as it has high v_r/v_l asymmetry. It is likely that if such habit is to be observed, a candidate would be melt-crystallized PVDF.

Re-entrant corners are quite common in twinned polymer crystals, e.g. in {110} or {310} twins of PE [5]. Sadler [3] has invoked their existence in support of his rough-surface non-nucleated growth theory. Toda [5] has noted a degree of in-filling of the re-entrant corner in {311} twins but not in {110} twins, attributing the former to a particularly narrow corner angle. However, to our knowledge there have been no reports of re-entrant corners in single crystals, other than those due to defects. Owing to the rather large angle of the predicted re-entrant corner such as in Fig. 3, and due to the small mean spreading distance of steps, we anticipate that the re-entrant corner would not fill in and should remain observable.

4. Conclusions

Calculated crystal shapes based on the proposed theoretical treatment of curved asymmetric faces give good agreement with experimentally observed habits of {110}-bound lozenge single crystals in long-chain *n*-alkanes and PVDF. The shape of the ''*a*-axis lenticular'' crystals [16], i.e. lens-shaped crystals with the long-axis parallel to *a*, is well reproduced. It is shown that the shape of an asymmetric lateral crystal face is defined by two kinetic parameters, v_r/v_l and $il_0^2/(v_r + v_l)$, rather than by just one parameter, $il_0^2/2v$, for a symmetric face. The observed dependence of the ratio of left- and right step propagation rates on supercooling is consistent with the general principles of crystallization kinetics. The high ratio of initiation-to-propagation steps, which leads to high curvature, gives a picture of a crystallization process that is under certain conditions only marginally nucleation controlled. The observed ten-fold difference between right- and left-moving steps on α-crystals of PVDF is most likely a consequence of the difference between edge-on and flat-on chain attachment at these steps, respectively. A combination of high asymmetry of step velocities and high nucleation-to-propagation ratio is predicted to potentially produce single crystals with re-entrant corners.

A similar analysis is in progress dealing with crystal habits of poly(ethylene oxide). This work will be published elsewhere [29].

Acknowledgement

The authors are grateful for financial support by the Engineering and Physical Research Council.

References

[1] Keith HD. J Appl Phys 1964;35:3115.
[2] Khoury F. Faraday Discuss Chem Soc 1979;68:404.
[3] Sadler DM. Polymer 1983;24:1401.
[4] Sadler DM, Gilmer GH. Polym Commun 1987;28:243.
[5] Toda A. Polymer 1991;32:771.
[6] Mansfield ML. Polymer 1988;29:1755.
[7] Point JJ, Villers D. J Cryst Growth 1991;114:228.
[8] Frank FC. J Cryst Growth 1974;22:233.
[9] Seto T. Rep Prog Polym Phys Jpn 1964;7:67.
[10] Lovinger AJ. Macromolecules 1996;29:8541.
[11] Toda A, Arita T, Hikosaka M. Polymer 2001;42:2223.
[12] Organ SJ, Keller A. J Mater Sci 1985;20:1571.
[13] Ungar G, Mandal PK, Higgs PG, de Silva DSM, Boda E, Chen CM. Phys Rev Lett 2000;85:4397.
[14] Putra EGR, Ungar G. Macromolecules 2003;36:3812.
[15] Putra EGR, Ungar G. Macromolecules 2003;36:5214.
[16] Ungar G, Putra EGR. Macromolecules 2001;34:5180.
[17] Ungar G, Putra EGR, de Silva DSM, Shcherbina MA, Waddon AJ. Adv Polym Sci 2005;180:45 [interphases and mesophases in polymer crystallization I].
[18] Shcherbina MA, Ungar G, in preparation.
[19] Shcherbina MA, Ungar G. Polymer 2006;47:5505.

[20] Tanzawa Y, Toda A. Polymer 1996;37:1621.
[21] Toda A. Faraday Discuss Chem Soc 1993;95:129.
[22] Kyu T, Mehta R, Chiu H-W. Phys Rev E 2000;61:4161.
[23] Higgs PG, Ungar G. J Chem Phys 2001;114:6958.
[24] Bunn CW. Trans Faraday Soc 1939;35:482.
[25] Hasegawa R, Takahashi Y, Chatani Y, Tadokoro H. Polym J 1972;3:600.
[26] Bachmann MA, Lando JB. Macromolecules 1981;14:40.
[27] Shcherbina MA, Ungar G. Macromolecules 2007;40:402.
[28] Geil PH. Polymer single crystals. New York: Wiley; 1963.
[29] Shcherbina MA, Ungar G, in preparation.
[30] Lotz B, Kovacs AJ, Bassett GA, Keller A. Kolloid Z Z Polym 1966; 209:115.
[31] Kovacs AJ, Gonthier A, Straupe C. J Polym Sci Polym Symp 1977; 59:31.